THE JOURNAL OF PHYSICAL CHEMISTRY C

ARTICLE

pubs.acs.org/JPCC

Wettability Control Mechanism of Highly Contaminated Hydrophilic Silica/Alumina Surfaces by Ethyl Cellulose

Shengqun Wang, Nataliya Segin, Ke Wang, Jacob H. Masliyah, and Zhenghe Xu*

Department of Chemical and Materials Engineering, University of Alberta, Edmonton, Alberta T6G 2G6, Canada

ABSTRACT: In a previous study (Feng et al. *Langmuir* **2010**, *26*, 3050), a biodegradable ethyl cellulose (EC) was proven to be an effective demulsifier for water-in-diluted bitumen emulsions by flocculation-enhanced coalescence through the displacement of protective interfacial films. In the current study, the potential of EC in displacing the asphaltene or bitumen layers adsorbed on hydrophilic silica and alumina surfaces is investigated in an attempt to explore the applicability of EC as a chemical modifier to control the wettability of solids contaminated by heavy oils. The quartz crystal microbalance with dissipation (QCM-D) was used to determine the adsorption of EC on silica or alumina which has a thin layer of asphaltene contaminant (preadsorbed). For comparison, the adsorption of asphaltenes on silica or alumina which was preadsorbed with EC was also determined. The effect of EC on the wettability and morphology of the asphaltene- or bitumen-contaminated (coated) silica or alumina surfaces was determined by contact angle measurement and atomic force microscope (AFM) imaging. The measurements were conducted before and after soaking the asphaltene- or bitumen-coated silica and alumina wafers in EC-in-toluene solution. The results of QCM-D showed irreversible adsorption of asphaltenes on silica surface. However, EC was found to adsorb on and/or displace the irreversibly preadsorbed asphaltenes from silica and alumina surfaces. Atomic force microscope imaging confirmed a gradual displacement of the preadsorbed asphaltenes or bitumen by EC from silica wafer surfaces, in which the asphaltene/bitumen contaminants were forced into sporadic larger aggregates. After 7 h of contact with EC-in-toluene solutions, the majority of the silica substrate surfaces precontaminated by asphaltenes or bitumen were covered with EC. Correspondingly, the contact angle of water decreased from about 88° and 67° of the original asphaltene- and bitumen-coated surfaces, respectively, to final values in the range of 20−30° which are similar to that of the EC-coated surface. Effect of EC adsorption on increasing the wettability of chemically hydrophobized (silanized) silica surface with water contact angle from 80° to 100°, is more conservative, leading to an intermediate water contact angle of 60−70° due to its weak binding and different conformations of EC on hydrophobic surfaces from that on hydrophilic surfaces. These findings demonstrated the possibility of using EC to modify the wettability of hydrocarbon-contaminated inorganic solids (clays) to improve heavy oil processing.

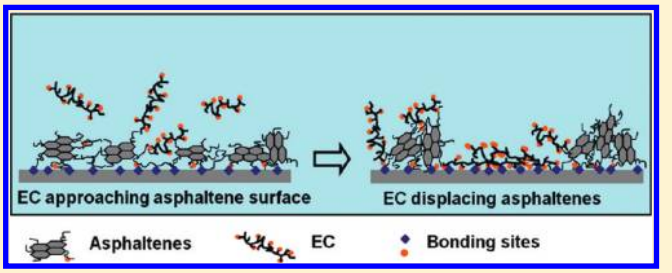

INTRODUCTION

Wettability of solids is known to play a critical role in many natural and industrial processes, in particular in the area of life science and nanotechnology. For example, protein adsorption is largely controlled by hydrophobic interactions which greatly depend on the wettability of the surface on which a protein adsorbs.[2,3] The design of a superhydrophobic surface similar to that of a lotus leaf is of special interest in nanotechnology for the development of self-cleaning materials.[4,5] During heavy oil processing, for example, two main challenges, demulsification of water-in-oil emulsions and removal of organic-contaminated solids, are also related to solid surface wettability. The organic-rich solids and emulsified water droplets, remaining in oil, are detrimental to downstream upgrading/refining operations and need to be removed from the oil phase.[6,7] Although chemical addition can be used to help break water-in-oil (w/o) emulsions,[8] solids removal usually depends on enhanced mechanical forces by, for example, centrifugation. The difficulty of both the emulsified water droplets and solids removal is magnified by the presence of an extremely viscous, solids-stabilized rag layer in the form of mixed emulsions.[9−12] In our previous study,[1] a biodegradable ethyl cellulose (EC) was found to be an effective demulsifier for breaking water-in-diluted bitumen emulsions.[1,13] The addition of EC to the organic phase was found to cause a significant reduction in diluted bitumen−water interfacial tension. Water droplets were shown to flocculate and coalesce in diluted bitumen solutions containing EC, depending on EC concentration. In this study, we investigated the potential of EC as a wettability modifier of solids from oil-wet to water-wet in the context of heavy oil processing. The effect of EC addition on the wettability of asphaltene- or bitumen-contaminated hydrophilic silica and alumina surfaces was determined by contact angle measurements. The mechanism of wettability alteration by EC addition was determined by atomic force microscope (AFM)

Received: October 2, 2010
Revised: March 11, 2011
Published: April 29, 2011

imaging before and after soaking the asphaltene- or bitumen-coated silica and alumina wafers in EC-in-toluene solution for varying periods of time. Below are introductions of the problematic organic-rich solids in heavy oil processing and the approach to selecting EC as a chemical modifier to control the solid wettability.

In heavy oil processing, the presence of oil-wet and biwettable solids usually causes the most challenging problems in water-in-oil (w/o) emulsions.[6,14−17] These solids can accumulate at water−oil interface to cause Pickering-enhanced stabilization of w/o emulsions. As measured by Wu et al. (2008), solids account for about 21 wt % of the interfacial materials that stabilize w/o emulsions.[18] A combination of asphaltenes and solids leads to the most stable w/o emulsions.[19−22] Fine water droplets stabilized by asphaltenes and oil-wet solids tend to accumulate between the bulk water and heavy oil (diluted-bitumen) phases, forming a distinct intermediate layer of extremely high viscosity. This layer is known as the rag (sludge) layer which hinders effective water−oil phase separation.[9,11,18,19,21,23] Oil-wet solids are naturally carried over to the oil phase from upstream operation. These solids may cause equipment fouling and/or catalyst poisoning in downstream refining process.[15] The organic-rich solids consist mainly of ultrafine aluminosilicate clay particles that are originally hydrophilic. Due to contact with heavy oil in the reservoir or during oil processing, a layer of "asphaltene-like" organic materials is adsorbed/anchored onto the surface of the initially hydrophilic solids, rendering the solid surface hydrophobic.[15,16] Other bitumen components such as resins can also adsorb on hydrophilic surfaces, but their adsorption could be highly reversible.[24] Asphaltene adsorption on hydrophilic surfaces is irreversible and the asphaltene-contaminated solids remain hydrophobic even after being washed with good solvents such as toluene or naphtha.[15,16] Removal of highly contaminated and hence hydrophobic solids can be extremely challenging even with centrifuges, since the particle size of clays can be as small as a few tenths of a micron.[6] It is therefore of great importance to increase the wettability of the contaminated (oil-wet) solids in an oil phase so that they can migrate to the aqueous phase without significant contribution to stabilization of w/o emulsions and any solids-related negative problems in downstream heavy oil upgrading and refining.

Adding a surface active chemical modifier can possibly make a solid surface more water-wettable. For a chemical modifier to increase the water-wettability of the organic-rich solids in heavy oil processing, it has to be soluble in the heavy oil for delivery through the oil phase. It can change the solid surface wettability either by adsorbing on top of the organic contaminants or by displacing them from the solid surface. For simple surface adsorption, the chemical modifier has to be amphiphilic and of large molecular weight so that its hydrophobic segments may bind with the organic contaminants on the solids surface. In this manner, the hydrophilic segments (groups) are exposed to the oil, leading to the formation of an outer-hydrophilic-layer on solids as schematically shown in Figure 1a. However, this conformation of chemical modifier is entropically unfavorable in a bulk oil phase in which most of the molecules are apolar. Preferably, the chemical modifier has functional groups that can compete for the hydrophilic binding sites on the solid substrate with the contaminating organic species, thereby displacing the organic contaminants from the solid surface, as schematically shown in Figure 1b. In this case, it is extremely important to control the number of hydrophilic groups of the chemical modifier's molecules so that a sufficient number of active

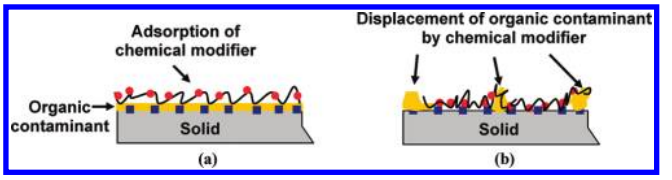

Figure 1. Effect of amphiphilic chemical modifier on an organic contaminated solid surface (red circles and blue squares are polar groups on chemical modifier and solid surface, respectively): (a) chemical modifiers adsorb on the top of organic contaminants through nonspecific interaction and leave the polar segments exposed; (b) chemical modifier displaces the organic contaminant and adsorb on the solid surface.

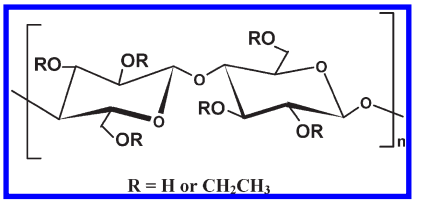

Figure 2. Molecular structure of ethyl cellulose (EC).

hydrophilic groups are available upon adsorption to make the solid surface hydrophilic. In general, an oil-soluble, amphiphilic modifier is needed to achieve this purpose. Specifically, a demulsifier that adsorbs at water−oil interfaces and displaces the interfacial film is a good candidate. In this condition, the demulsifier weakens the interfacial film by penetrating into the film and displacing the interfacial materials while its presence at the interface cannot provide enough protection from water droplet flocculation and/or coalescence.[8] The same mechanism can be applied to a solid−oil interface for solid wettability modification because fundamentally the water−oil and hydrophilic solid−oil interfaces are similar. At the solid−oil interface, the demulsifier needs to access the polar binding sites such as −OH groups on the hydrophilic silica and alumina surfaces and then displaces the organic contaminants off the solid surfaces, a process similar to those that occurred at a water−oil interface. On the basis of this scenario, an appropriate demulsifier should modify both the surface properties of the solids in the bulk oil phase and the water−oil interfacial properties, which benefits both the demulsification of w/o emulsions and the breaking of rag layers.

As reported previously, EC is an effective demulsifier for water-in-diluted bitumen emulsions.[1,13] EC displaces the protective interfacial film at the water−oil interface and induces a flocculation-enhanced coalescence of water droplets. EC is a linear polymer with a backbone of cellulose structure (Figure 2). The side hydroxyl groups on the backbone are partly substituted by ethoxyl groups, making EC oil-soluble while maintaining its amphiphilic nature. EC can adsorb on a hydrophilic solid surface through hydrogen bonds between hydroxyl groups and oxygen atoms in EC chains and on solid surfaces. The ethoxyl side groups are relatively short, randomly distributed along the molecular chain, and separated by a linkage oxygen atom between glucose rings such that the intermolecular association of EC molecules is minimized to avoid the formation of hydrophobic layers once adsorbed on solid surfaces. These molecular characteristics of EC make it an ideal candidate for our purpose of exploring its ability to increase the water-wettability of heavy oil-contaminated solids in heavy oil processing.

EXPERIMENTAL SECTION

In the current study, silica and alumina were chosen as the solid surfaces to be investigated as they represent the basic components of clays. Asphaltenes represent the heaviest components of heavy oil and are known to be the major components contaminating solids in heavy oil. Asphaltenes were therefore used as the organic material to contaminate solid surfaces. Bitumen was also used as the organic contaminant in order to test if the results obtained by using asphaltenes can be extended to bitumen. A quartz crystal microbalance with dissipation function (QCM-D) was used to determine the adsorption of EC in toluene solutions on asphaltene preadsorbed (contaminated) silica and alumina surfaces. During the soaking experiments, hydrophilic silica or alumina wafers were dip-coated (contaminated) with a layer of asphaltenes or bitumen, and then immersed in EC-in-toluene solutions for a varying period of time. The contact angle of a water droplet on the treated wafer surfaces was measured and the nanoresolution morphology of the treated wafer surfaces was determined by AFM. All of the experiments were conducted to explore the potential of EC in increasing the water-wettability of the organic-contaminated solids in heavy oil.

Materials and Chemicals. Asphaltenes in vacuum distillation feed bitumen, provided by Syncrude Canada, Ltd., were precipitated at a 40:1 volume ratio of *n*-heptane/bitumen.[25] The heptane-precipitated asphaltenes account for ~11 wt % of bitumen. Ethyl cellulose (EC), purchased from Sigma-Aldrich, was used as received. The ethoxyl content of EC is 48 wt % and the molecular weight, determined by intrinsic viscosity measurement, is 46 kDa.[13] HPLC grade toluene, purchased from Fisher Scientific, was used as the solvent. Three types of alkylchlorosilanes (dimethyldichlorosilane, butyltrichlorosilane, and octyltrichlorosilane) from Fisher Scientific were used as silane coupling agent to modify the hydrophilic silica surface to become hydrophobic. Milli-Q water with a resistivity of 18.2 MΩ·cm, prepared with an Elix 5 system followed by purification with a Millipore-UV plus system, was used in the water contact angle measurements.

Silica wafers with one side being polished to a molecular level smoothness, purchased from NanoFab (University of Alberta, Canada), and C-plane alumina wafers (University wafer, Massachusetts, USA) were used as the model solid surfaces to represent building blocks of clays. Prior to their use, silica wafers were cut into 1 cm by 1 cm square pieces and cleaned in a 70 vol % sulfuric acid (98 vol % water solution) and 30 vol % hydrogen peroxide (30 wt % water solution) mixture at 85 °C for 25 min, followed by thorough washing with Milli-Q water and blow-drying with nitrogen. The alumina wafers were also cut into 1 × 1 cm pieces and immersed in the sulfuric acid for 10 min to remove organic contaminants, followed by thorough washing with Milli-Q water and blow-drying with nitrogen. The alumina wafers were then exposed to UV radiation in air (Bioforce Nanosciences, US) for 10 min. The silica and alumina surfaces cleaned as such are hydrophilic with a contact angle of water droplets less than 10° as measured by a drop shape analyzer (DSA100, Krüss, Germany).

Preparation of Hydrophobic Silica Surfaces. To evaluate the effect of EC on the wettability of the chemically hydrophobized solid surfaces, the hydrophilic silica wafers were hydrophobized chemically by immersion in 5 mM alkylchlorosilane-in-toluene solution for 12 h. The chlorosilanes chemically bond to hydroxyl (−OH) groups on hydrophilic silica surfaces, leaving the alkyl groups extending from the solid surface and thus making the surface hydrophobic. Thus prepared hydrophobic surfaces are stable in toluene due to covalent coupling of chlorosilanes with the −OH groups on solid surfaces.[26] The silanized silica wafers were found to be highly hydrophobic with contact angles of water from 80° to 102°.

Quartz Crystal Microbalance-Dissipation (QCM-D). QCM-D (Q-sense E4 system, Sweden) was used to measure the adsorption of asphaltenes and EC on quartz crystal sensors. The quartz crystals of 14 mm in diameter used in this study were AT-cut crystals (5 MHz) coated with silica (QSX 303) or alumina (QSX 309). A quartz crystal sensor is a thin piezoelectric plate with gold electrodes on each side.[24] When an ac voltage is applied to the electrodes, the crystal oscillates at a specific resonance frequency that is highly sensitive to the total mass of the crystal. When a mass is added to the sensor due to material adsorption, the resonance frequency of the sensor will decrease. The mass uptake on the sensor surface can be calculated by measuring the decrease of the frequency, Δf, in Hz. If the adsorbed layer is thin and rigid, the Sauerbrey relation is applicable. In this case, the decrease in resonance frequency is proportional to the mass uptake due to material adsorption:[24,27,28]

$$\Delta m = -\frac{C \times \Delta f}{n} \quad (1)$$

where Δm is the adsorbed mass (mass uptake) in mg/m^2, n is the number of harmonic overtones of the crystal sensor (n = 1, 3, 5, ..., 13), and C is a constant of the crystal. For the 5 MHz quartz crystal manufactured by Q-sense (Sweden), C = 0.177 mg/(Hz·m^2). This type of quartz crystal sensor was used in this study.

In addition to determining the quantity of the adsorbed mass, the QCM-D also monitors the dissipation, D, which is a measurement of energy loss due to viscous dissipation when oscillating the adsorbed materials with the crystal. Shifts in D during adsorption provide an indication of the rigidity of the adsorbed layer. A small dissipation shift indicates a rigid and compact adsorbed layer.[29] A combination of the shifts in f and D is generally used to determine whether the Sauerbrey relation is valid or not. As a rule of thumb, the Sauerbrey relation of eq 1 is applicable when $\Delta D/\Delta f < 0.2 \times 10^{-6}$/Hz.[30] Furthermore, a plot of ΔD versus Δf provides information about adsorption kinetics and structural changes of adsorbed layers over time, which provides a better interpretation of the frequency shift than simply mass uptake.[28]

Prior to each QCM-D experiment, the quartz crystal sensor was soaked in ethanol and sonicated for 10 min, followed by thorough rinsing with Milli-Q water and blow-drying with nitrogen. The sensor was then exposed to UV radiation in air for 10 min. The treated sensors bear a layer of hydroxyl groups and have a water contact angle of less than 10°. Since the experiments were carried out in toluene, solvent-resistant Kalrez O-rings and gaskets and GORE pump tubing (100CR) were used.

To start a QCM-D experiment, a clean crystal sensor was carefully inserted in the flow module with the active surface facing the testing solutions. The flow module was mounted on the chamber platform, and the toluene solution was pumped through the flow module by an IPC-N peristaltic pump (Ismatec, Switzerland) at a flow rate of 200 μL/min. This flow rate was chosen as higher flow rates would lead to noticeable noises in frequency (e.g., frequency fluctuation is about 1 Hz), causing interferences in quantitative analysis of the recorded signals. The variation of the temperature of the solution was controlled to be within 0.02 °C by a built-in heating and cooling thermoelectric device under the flow module in the chamber platform. For each

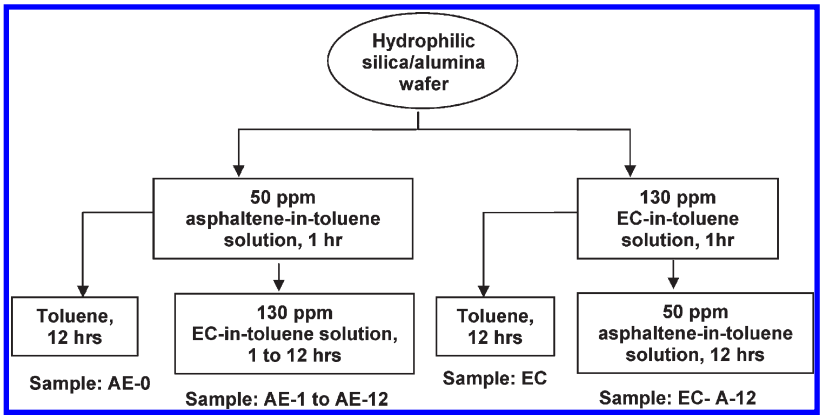

Figure 3. Soaking experiment procedures and corresponding sample codes. Note: To prepare a bitumen-coated surface, replace 50 ppm asphaltene-in-toluene solution with 500 ppm bitumen-in-toluene solution and follow the same experimental procedures with samples being coded as BE in place of AE.

run, pure toluene was first pumped through the system until a stable baseline was obtained. Then 50 ppm asphaltene-in-toluene solution was introduced to the flow module. The adsorption of asphaltenes on the sensor surface caused a negative shift (decrease) in frequency and a positive shift (increase) in dissipation. After the adsorption reached equilibrium as judged by a frequency shift less than 1 Hz in 10 min, the sensor surface was washed by switching the asphaltene solution to pure toluene to remove any loosely adsorbed asphaltenes. Then the EC-in-toluene solution was pumped through the system in order to study the adsorption of ethyl cellulose (EC) on the sensor surface with preadsorbed asphaltenes. EC was allowed to adsorb on the preadsorbed asphaltenes and/or displace the preadsorbed asphaltenes from the sensor surface until a new equilibrium was reached. For comparison, EC adsorption from toluene solutions on fresh sensor surfaces followed by the adsorption of asphaltenes was also measured. All QCM-D adsorption experiments were carried out at 22.00 ± 0.02 °C.

During the QCM-D experiment, the frequency and dissipation shifts of all the seven harmonics (n = 1, 3, 5, ..., 13) were recorded. For the sake of simplicity, only two harmonics (n = 3 and n = 9) are shown in the results. In this study, we used the third overtone to determine the frequency and dissipation shifts and to calculate the corresponding mass uptake.

Soaking Experiment. In order to understand the wettability alteration mechanism of asphaltene- and bitumen-contaminated solids by EC adsorption, soaking experiments were carried out using procedures schematically described in Figure 3. In each test, silica or alumina wafers (1 cm by 1 cm) were immersed in 50 ppm asphaltene- or 500 ppm bitumen-in-toluene solutions for 1 h, after which they were removed from the toluene solution and rinsed with about 20 mL of pure toluene to wash away any residual asphaltene/bitumen solutions and/or loosely attached asphaltenes/bitumen. The asphaltene- or bitumen-coated (contaminated) wafers were then immediately soaked in 130 ppm EC-in-toluene solutions for a varying period of time from 1 to 12 h. The samples were then taken out of the EC solution, rinsed with toluene, and then blow-dried with nitrogen. Sampling in a time domain (i.e., as a function of time) in EC solution allows one to follow up the structural changes of the asphaltene/bitumen layers preadsorbed on hydrophilic solid surfaces. For the convenience of discussion, the samples were coded as follows: AE-i for asphaltene-coated surface soaked in EC solution, with i representing the amount of time (in hours) that the sample was soaked in EC solution (i = 0, 1, 2, 3, 4, 5, 6, 7, and 12 h); and BE-i for bitumen-coated surfaces soaked in EC solution for i = 0, 1, 2, 3, 4, 5, 6, and 7 h. The soaking experiment was carried out at room temperature (21.0 ± 0.5 °C).

As a control to study the stability of immobilized asphaltenes and bitumen on hydrophilic wafer surfaces, an asphaltene- or bitumen-coated wafer was placed in pure toluene for 12 h. Control tests were also conducted by immersing a bare wafer in 130 ppm EC-in-toluene solution for 1 h, followed by soaking in pure toluene for 12 h. To study the effect of asphaltenes on the EC-coated solid surface, the EC-coated wafer obtained here was placed in 50 ppm asphaltene- or 500 ppm bitumen-in-toluene solutions for 12 h.

The prepared surfaces were characterized by contact angle measurements and AFM imaging. Water contact angle was measured to determine changes in the surface wettability as a consequence of compositional and conformational change of the organic contaminants on the hydrophilic solid surface. Topographical images of different samples, obtained by AFM, were used to observe changes in the structure of the surface layer.

Contact Angle Measurements. Static contact angles of water on sample surfaces were measured using a drop shape analyzer (DSA100, Krüss, Germany) equipped with an optical microscope and illumination system. The sessile drop method with drop volumes of 10−20 μL was employed at room temperature (21.0 ± 0.5 °C). Contact angles from both the left and right three-phase contact points of the water droplet were determined, and the average value was used. For each sample, measurements were performed at three locations with at least six measurements at each location. Standard deviations of the measurements were calculated and shown as error bars in the respective figures.

Atomic Force Microscope (AFM) Imaging. AFM topographical images of the sample surfaces were obtained using an Agilent 5500 Molecular Imaging Microscope (Agilent Technologies, Inc., Chandler, AZ) operated under AAC mode in air using silicon nitrate cantilevers (RTESP, Veeco, Santa Barbara, CA), with a nominal resonance frequency of 200−300 kHz. During AFM imaging, the amplitude set point (A_s) was set at 95−98% of the free amplitude (A_0). At this ratio of A_s/A_0, the force applied by the cantilever tip on the sample surfaces was sufficiently low to avoid damaging the sample surfaces. Multiple locations were imaged for all of the samples at room temperatures (21.0 ± 0.5 °C), and a representative image was presented.

RESULTS AND DISCUSSIONS

Adsorption of EC on Asphaltene Preadsorbed Surfaces. The adsorption of EC on asphaltene preadsorbed (contaminated) silica surface is shown in Figure 4a. It shows that adsorption of asphaltenes on silica surface led to a decrease of frequency by about −43 Hz and an increase in dissipation by $\sim 2.0 \times 10^{-6}$. Adsorption reached equilibrium after 1 h, indicating a slow adsorption process characteristic of large asphaltene molecule systems. After the sample was rinsed with toluene for 30 min, a slight increase in the frequency and decrease in the dissipation were observed, indicating an insignificant effect of solution viscosity on the frequency drop and possible removal of loosely adsorbed asphaltenes from the surface. Since the changes in frequency and dissipation are not significant during toluene rinsing, most of asphaltenes on the solid surface are considered irreversibly adsorbed. The ratio of the dissipation shift to the frequency shift, $\Delta D/\Delta f$, is quite low ($<0.2 \times 10^{-6}$/Hz), indicating that the adsorbed asphaltene layer is rigid and Sauerbrey relation of eq 1 is valid. Similar observations were reported by other researchers.[24,27,31,32] Since the concentration of asphaltene-in-toluene solution is very low (50 ppm), the viscosity and density of the solution can be approximated by the values of the pure solvent, i.e., toluene.[31] At equilibrium, the amount of asphaltenes adsorbed was calculated to be ~ 7 mg/m^2, comparable to the values reported for similar systems.[24,32]

As also shown in Figure 4a, the contact with EC solutions of silica sensor surfaces preadsorbed with a layer of asphaltenes caused a further decrease in resonance frequency and increase in dissipation. The changes of f and D were fast in the first 4 h after introducing EC solution, followed by a slow evolution. The overall shift in frequency and dissipation after introduction of EC are about −50 Hz and 4.5×10^{-6}, respectively. Using eq 1, the total mass uptake (asphaltenes+EC) on the sensor surface is calculated to be about 15.5 mg/m^2. An interesting observation is the distinct dissipation shift of the lower overtones ($n = 3$), D_3, after introduction of EC. The dissipation of the third overtone first increased to a larger degree and then decreased gradually to the level of the higher order overtones ($n = 5-13$) as represented by D_9 in Figure 4a. It is well documented that the lower order overtones are more sensitive to the outer region of the adsorbed layer (regions far away from the solid surface).[27] The characteristic changes in the dissipation of the third overtone indicate that, shortly after EC solution was introduced, the outer region of the film was softer than the inner region. The softness of the outer region of the film can be attributed to the adsorption of EC, structural changes, and/or trapping of the solvent with increased roughness of the film−liquid interface due to EC adsorption. With increasing contact time with EC solutions, the outer region of the film gradually became as rigid as the inner region, leading to a more homogeneous film across the thickness of the film. It should be noted that the results from the QCM-D tests could not distinguish whether EC simply adsorbed on preadsorbed asphaltenes or displaced them. Such information can be derived from the soaking experiments to be described later.

Similar results were obtained using an alumina-coated quartz crystal sensor as shown in Figure 4b. Considering similar surface characteristics of silica and alumina in toluene (e.g., both bear hydroxyl functional groups), this observation is not unexpected. The calculated mass uptakes of asphaltenes and asphaltenes+EC are 6.2 and 14.3 mg/m^2, respectively. Over the duration of the experiment, the subtle change in dissipation profile of the third overtone as observed in Figure 4a for silica surface was absent, indicating that the build-up of EC films on asphaltenes preadsorbed on alumina is more uniform than that on the silica surface.

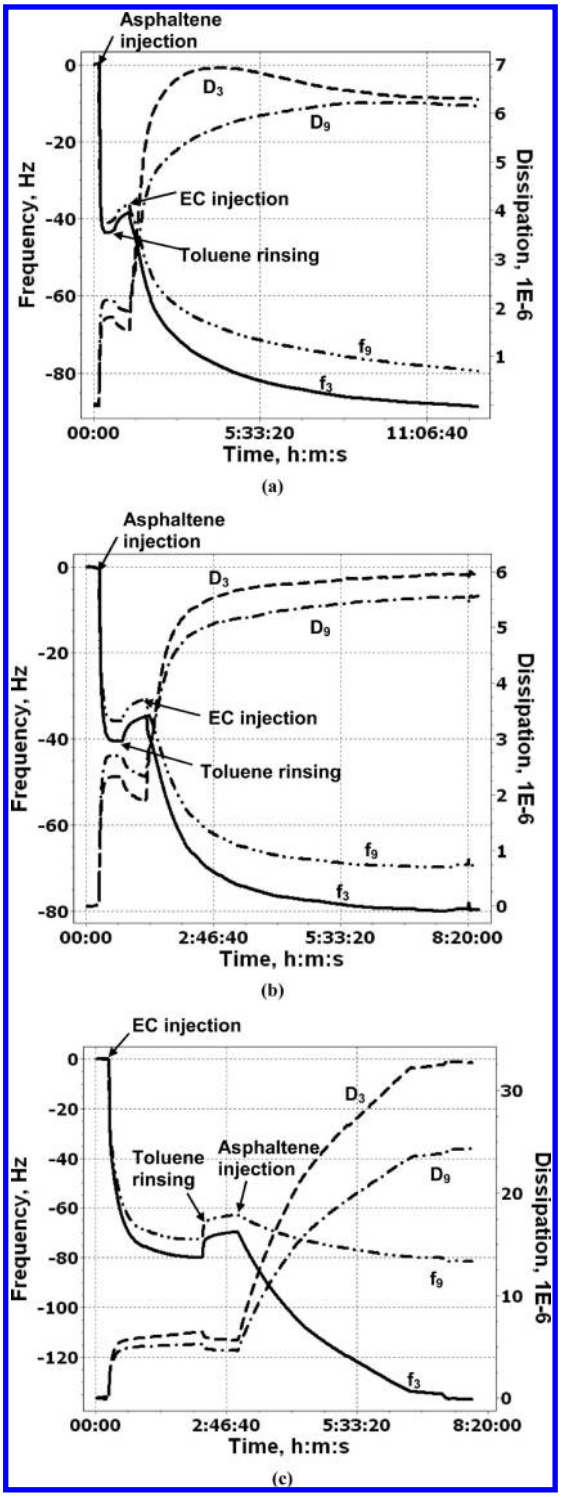

Figure 4. Frequency and dissipation shift as a function of adsorption time in QCM-D experiments: (a) EC adsorption on asphaltene-coated silica surface; (b) EC adsorption on asphaltene-coated alumina surface; (c) asphaltene adsorption on EC-coated silica surface.

Adsorption of Asphaltenes on EC Preadsorbed Surfaces. Figure 4c shows that direct adsorption of EC on a hydrophilic silica surface caused a frequency shift of −70 Hz and a dissipation shift of 5.5×10^{-6}, corresponding to a mass uptake of 12.5 mg/m^2 (density and viscosity of toluene were used in the calculation since 130 ppm EC-in-toluene solution is quite dilute). Rinsing with pure toluene caused only a small increase in f and drop in D, indicating that most EC is irreversibly adsorbed on the hydrophilic silica surface. Subsequent adsorption of asphaltenes caused a large decrease of frequency for the lower order overtones (Δf_3 = −70 Hz). Apparently, it seemed that a large amount of asphaltenes was adsorbed on the EC surface. Accompanied with asphaltene adsorption, a large increase in dissipation was also observed ($\Delta D_3 = 26 \times 10^{-6}$), indicating a much softer and more rugged asphaltene film. What's more, the frequency shifts of the higher order overtones are quite small in comparison with Δf_3 (Δf_9 = −17 Hz), indicating a more heterogeneous film from the inner to the outer region away from the solid substrate. As revealed by AFM imaging to be discussed later, asphaltenes only randomly adsorbed on EC surface in the form of separate aggregates. Such a layer is rough and would trap a large amount of toluene, which is likely the cause of both larger dissipation and frequency shifts.[28,29]

The mass uptake, Δm, in each adsorption event calculated by the Sauerbrey equation is shown in Figure 5. For EC adsorption after asphaltenes on silica, the total mass uptake of asphaltenes+EC is about 15.5 mg/m^2. However, for EC adsorption directly on silica surface, the mass uptake is about 12.5 mg/m^2. The total mass uptake on silica in the two adsorption events is comparable. The mass uptake on alumina surface of asphaltenes+EC is similar to that on a silica surface.

To extract more structural information of the film during the adsorption process, the ΔD versus Δf was plotted in Figure 6, in which only the values of the third overtone were shown. For asphaltene adsorption on hydrophilic silica and alumina surface, the slopes of $\Delta D/\Delta f$ were very small, indicating the formation of a dense adsorbed layer on these two hydrophilic solid surfaces. Subsequent adsorption of EC caused only a slight increase in the slope values, ensuring the applicability of the Sauerbrey relation. With continuous adsorption of EC, the slope of $\Delta D/\Delta f$ decreased gradually, indicating an increasingly more rigid film due to increased packing of adsorbed molecules. For EC adsorption on a bare silica surface, the $\Delta D/\Delta f$ simulates the case of EC adsorption on asphaltene preadsorbed silica surface with comparable ΔD and Δf values being reached, which implies similar final film properties in these two adsorption events of EC. This finding suggests that whether EC adsorbed on asphaltene preadsorbed silica surface or directly on the bare silica surface, the adsorbed film would eventually become dominated by EC. Adsorption of asphaltenes on the EC surface, on the other hand, led to a larger slope value for $\Delta D/\Delta f$, indicating a much more loosely adsorbed asphaltene layer than that adsorbed directly on silica or alumina surfaces. The distinct linear relationship between ΔD and Δf suggests that there is no conformational change during adsorption of asphaltenes on EC.[33]

Water Wettability of Sample Surfaces. Contact angles of water on the surfaces prepared by soaking experiments are shown in Figure 7. A bare silica surface had a water contact angle of less than 10°. Upon adsorption of asphaltenes or bitumen, the water contact angle increased to 88 ± 2° for asphaltenes and 67 ± 2° for bitumen. This asphaltene or bitumen layer is considered to be irreversibly adsorbed on silica as it did not dissociate from the silica surface after soaking in toluene for 12 h. After samples were soaked

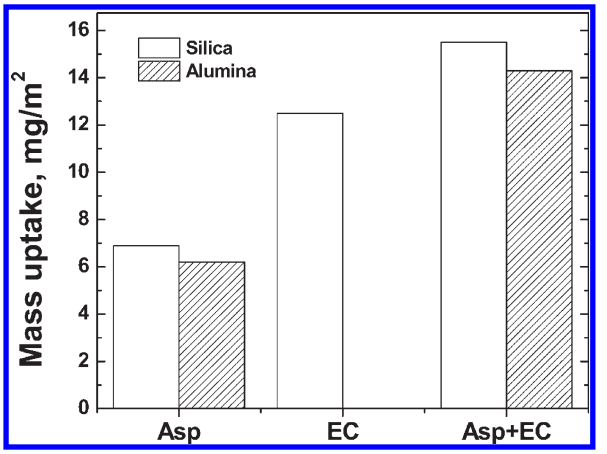

Figure 5. Mass uptake on a QCM-D sensor surface in each adsorption event in Figure 4.

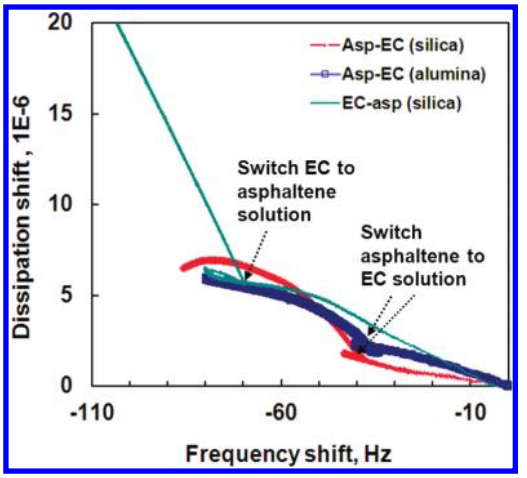

Figure 6. $D-f$ plot of the QCM-D adsorption results in Figure 4.

in EC-in-toluene solution, however, the water contact angle on the asphaltene- and bitumen-coated surfaces decreased significantly, indicating a change to a more water-wettable surface. The water contact angle reduced rapidly in the first 4 h, followed by a gradual reduction and finally leveled off after 7 h at a value of 25−30°. Such a contact angle value is comparable to that of water on an EC-adsorbed silica surface (∼20°). These observations suggest an "EC-like" surface be obtained after exposure of the asphaltene or bitumen preadsorbed surfaces to EC solutions. Such a finding is consistent with the conclusions derived from the adsorption measurement using QCM-D (Figures 4a, 5, and 6). Similar results were obtained for the alumina surface with preadsorbed asphaltenes (Figure 7c). The decrease in the water contact angles was more rapid for bitumen-coated surfaces than that for asphaltene-coated surfaces, indicating a competitive but reversible adsorption of resins together with asphaltenes during bitumen adsorption. Quantitatively, one can use the Cassie equation given below to estimate the coverage of asphaltenes or bitumen on the solid surface as a function of soaking time to EC solutions.

$$f_{AB}(t) = \frac{\theta(t) - \theta_{EC}}{\theta_{AB} - \theta_{EC}} \quad (2)$$

where $f_{AB}(t)$ is the fraction coverage of asphaltenes or bitumen at soaking time t to the EC solution, $\theta(t)$ is the contact angle

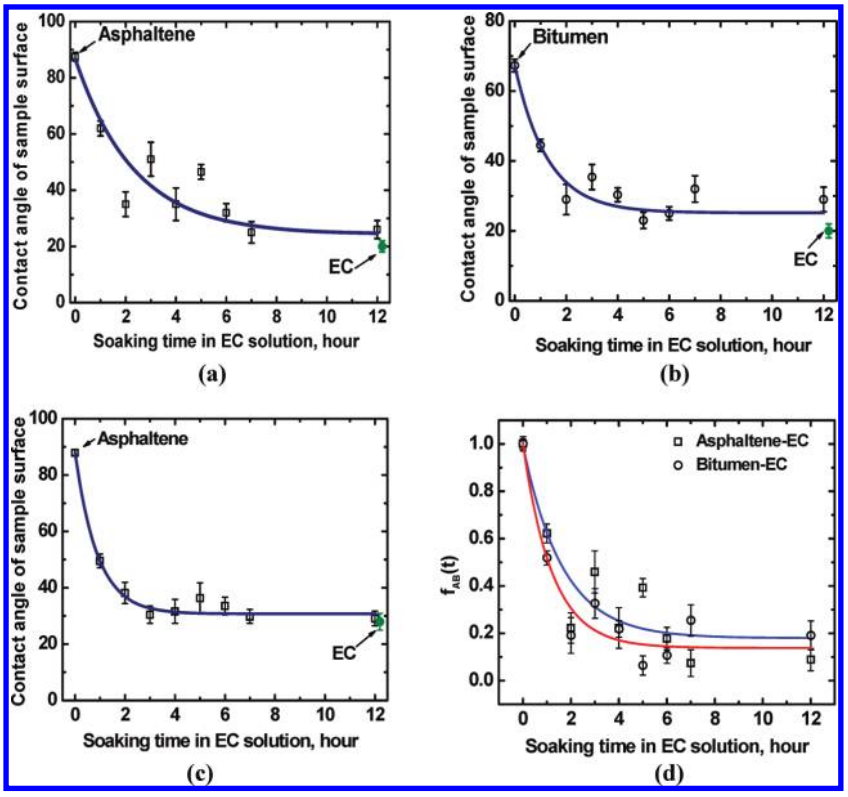

Figure 7. Water contact angles (deg) of a sample surface after soaking in EC-in-toluene solutions (scatters, experiment data; lines, fitted lines by exponential decay model): (a) asphaltene-coated silica surfaces; (b) bitumen-coated silica surfaces; (c) asphaltene-coated alumina surfaces; (d) $f_{AB}(t)$ profiles of plots (a) and (b) with the exponentially fitted curves by eq 2.

Table 1. Fitting Parameters of Figure 7d by Exponential Equation 3

parameters	asphaltenes−EC	bitumen−EC
A_0	0.82	0.86
α	0.60	0.82
Y_0	1.65	1.22

measured at soaking time t, and θ_{EC} (=20°) and θ_{AB} (=88° or 67°) are the contact angles of water on EC and asphaltene- or bitumen-covered surfaces, respectively. The calculated $f_{AB}(t)$ profiles as a function of soaking time to EC solutions shown in Figure 7d can be well described by an exponential function of eq 3 below, represented by the fitted curve in the figure.

$$Y = A_0 \exp(-\alpha x) + Y_0 \quad (3)$$

The decay parameter α for bitumen film (α = 0.82) is higher than that for asphaltene film (α = 0.60) (Table 1), suggesting that bitumen films are easier to be displaced by EC than asphaltene films or that EC adsorbs more readily on bitumen film than on asphaltene films. Both EC adsorption events follow a first-order rate process. To distinguish whether displacement of adsorbed film by EC or EC adsorption on the preadsorbed asphaltene or bitumen films is responsible for the observed increase in water wettability, AFM imaging was performed.

Topography of Sample Surfaces. Topographical images of the sample surfaces with hydrophilic silica as substrate in the soaking experiments are shown in Figure 8. Images of AE0 (asphaltene-coated surface, Figure 8a) and BE0 (bitumen-coated surface, Figure 8b) show typical topographical features of asphaltenes and bitumen adsorbed on a hydrophilic silica surface; both asphaltenes and bitumen are randomly distributed in the form of closely packed colloid-like nanoaggregates, with an average root mean square roughness of ~1 nm.[1,34] In contrast, the image of EC (Figure 8c) shows a more uniform and much flatter surface morphology with an average surface roughness less than 0.5 nm, comparable to the roughness of the silica wafer itself.

Surface topography of asphaltene-coated surfaces as a function of soaking time in EC solutions is shown in Figure 8a (images AE-1 to AE-5 not shown). With increasing soaking time, surface topography of asphaltene films on silica shows two distinct changes: some aggregates grew in size while the discrete flat areas expanded on the surface. These two changes are much clearer in image AE-7 (7 h of soaking time), showing higher rough domains (the larger aggregates) and much expanded flat open areas. The AFM images suggest that EC displaced asphaltenes by pushing them to form larger aggregates.

The same phenomena are expected to occur on alumina surfaces due to similarity of the surface chemistry of alumina with that of silica. At neutral state, the hydrophilic alumina surface also has a layer of hydroxyl groups (Al−OH),[35] which makes hydrogen bonding possible during adsorption of asphaltenes or EC and displacement of asphaltenes by EC.

The effect of EC on bitumen-coated surfaces is very similar to that of asphaltene-coated surfaces, but the displacement process of bitumen by EC is faster. As seen in Figure 8b, after soaking in EC solution for 6 h, large bitumen aggregates were formed on the surface (BE-6). After 7 h of soaking, only a few bitumen aggregates were observed, implying that bitumen nearly completely detached

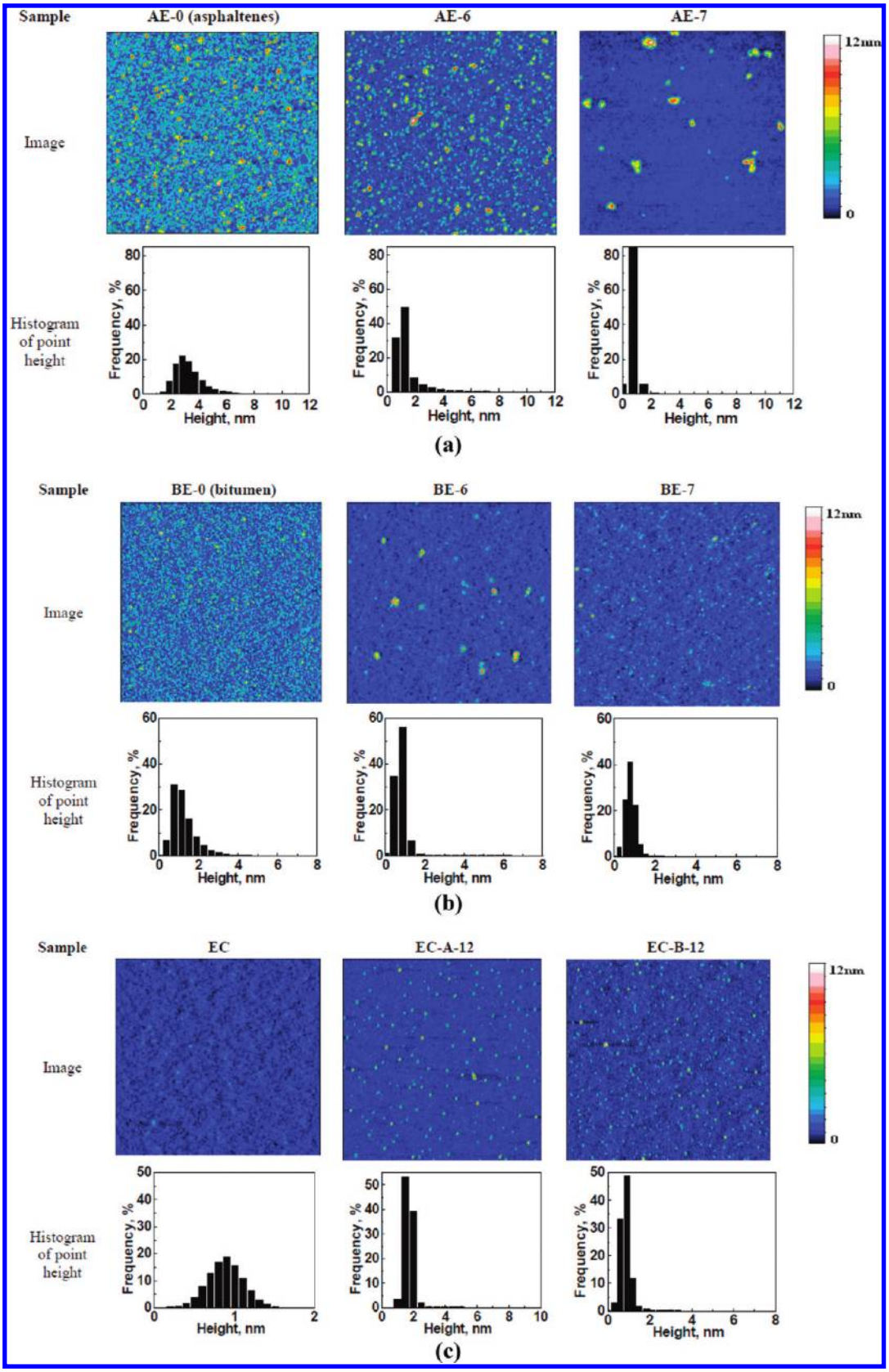

Figure 8. AFM topography images of the samples in soaking experiment: (a) asphaltenes and AE-*i* (asphaltene-coated sample surface soaked in EC-in-toluene solution for *i* hours, *i* = 0, 6, and 7); (b) bitumen and BE-*i* (bitumen-coated sample surface soaked in EC-in-toluene solution for *i* hours, *i* = 0, 6, and 7); (c) EC (EC-coated sample surface), EC-A-12 (EC-coated sample surface soaked in asphaltene-in-toluene solution for 12 h), and EC-B-12 (EC-coated sample surface soaked in bitumen-in-toluene solution for 12 h). The dimension of images is 2 μm × 2 μm.

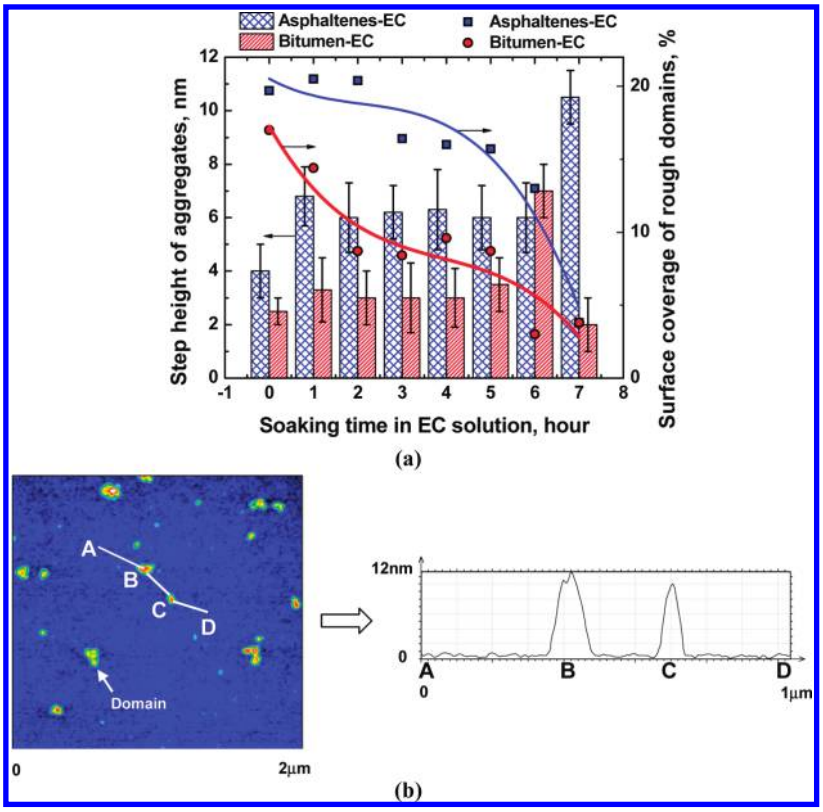

Figure 9. Statistical analysis of the AFM images in Figure 8: (a) step height of the aggregates (columns) as a function of soaking time in EC-in-toluene solution and surface coverage of the domains with height >0.5 nm (dots, calculated data from images; lines, polynomial fitting curve); (b) step height profile across asphaltene (bitumen) domains (A, B, C, and D correspond to four locations on the image along the line A → B → C → D).

from the solid surface (BE-7). This observation was not unexpected since bitumen contains many of the smaller polar molecules such as resins. Resins are able to adsorb on hydrophilic silica surfaces, but this adsorption is mostly reversible,[24] indicating that bitumen would be more easily displaced by EC.

Another control experiment was carried out to show the irreversibility of the displacement of asphaltenes and bitumen by EC. Here, a silica wafer was first coated by a layer of EC and then soaked in asphaltene- or bitumen-in-toluene solution for 12 h. The AFM images of the two samples in Figure 8c (EA-12 and EB-12) show only sparsely scattered aggregates of asphaltenes or bitumen on EC surfaces. The lateral size of these aggregates is in tens of nanometers with a height of a few nanometers. These observations are in agreement with the results from the QCM-D adsorption experiments which suggested a rough and loosely adsorbed asphaltene layer (Figures 4c and 6). Despite of asphaltene adsorption, the contact angle of the surface remains quite low, being 16.2 ± 2.7°. As we can note here, although the EC-coated surface had a low water contact angle (Figure 7), there was little asphaltene adsorption on EC and the adsorption is probably physisorption, which will be explained in the discussion section.

In order to analyze the displacement process in more detail, a statistical analysis of the surface features of the images was performed. Histograms of the data point height on each sample surface were obtained using image analysis software of the AFM instrument, and they are shown under each image. For the asphaltene surface (image AE-0 in Figure 8a), the aggregate height distribution has a broad peak at 2.9 ± 1.6 nm. With increasing soaking time, the distribution of the histogram began to develop in two manners: first, the distribution peak became narrower and higher and shifted to the left (flat area), indicating that the flat area began to dominate on the surface; second, the height of rough domains shifted further to the right, a sign that the aggregates grew in height. The flat area on the surface is considered to be locations where EC dominates. Figure 9a shows the step height distribution and the calculated surface coverage of the rough domains (asphaltene or bitumen aggregates). The step height distribution of the aggregates was estimated by drawing a line across the large domains as shown in Figure 9b and statistically analyzing the step heights using the image analysis software of the AFM equipment. It is observed that increasing soaking time led to a decrease in the surface coverage of the rough domains from ~20% (AE-0, BE-0) to ~4% (AE-7, BE-7), accompanied by a slow increase up to 6 h and a sharp increase between 6 and 7 h of soaking time of the rough domain heights. This sudden increase in the domain height of the aggregates coincides with a drastic breakdown of asphaltene layers, as indicated by a clear separation between the flat areas and domains.

Discussions on Displacement Process of Asphaltenes/Bitumen by EC. Combining the QCM-D, water contact angle, and AFM imaging results, a process of EC displacing asphaltenes from the silica surface, illustrated in Figure 10, is suggested. Two processes are highlighted. Initially, the EC molecules, being more surface active than asphaltenes, adsorb on the surface and at the defects of the asphaltene layers. The initial adsorption of EC accounts for a quick uptake of EC on asphaltene preadsorbed silica sensors in QCM-D and the corresponding rapid decrease in contact angle of water on asphaltene films with soaking time. In

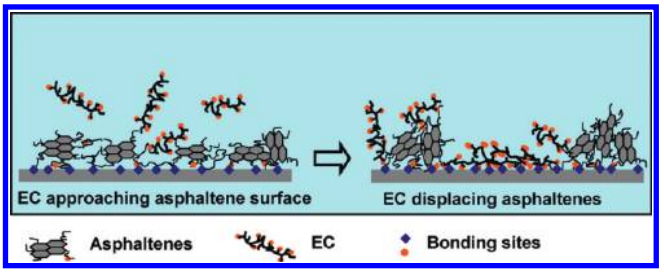

Figure 10. Schematics of asphaltenes displacement by EC on a hydrophilic solid surface.

this stage of EC adsorption, no significant change of the surface topography was observed by AFM imaging. Following this initial EC adsorption, a displacement process occurs, in which the adsorbed EC penetrates the asphaltene films and weakens the binding between asphaltenes−asphaltenes and asphaltenes−substrates, and gradually squeezes the asphaltene aggregates into small areas of larger size domains of significantly larger thickness. During the displacement process, the adsorbed asphaltenes are unlikely to lose quickly all their bonds with the silica surfaces due to the cross-link nature of asphaltene films similar to that formed at w/o interfaces,[8,36−38] leading to a slow shrinkage in contact area of asphaltenes with silica surfaces, as shown in the AFM images. A clear separation of asphaltene domains was observed when EC finally breaks all the connections between asphaltenes−asphaltenes and asphaltenes−substrates (e.g., image AE-7 in Figure 8a). The QCM-D tests showed no sign of asphaltenes detaching from the solid surface; instead there was a continuous increase in the uptake of material on asphaltene-adsorbed sensor surfaces. This is another sign that the adsorbed asphaltenes are likely pushed into larger size aggregates in the form of "islands" sporadically distributed on the silica surface. It is of course quite possible that stronger adsorption of EC may partially compensate for the loss of asphaltenes from sensor surfaces, exhibiting an overall increase in the mass uptake on the sensor surface. During the displacement process, the water contact angle of the sample surface continued to decrease gradually until leveling off at a value similar to that of EC-coated silica surface.

Figure 10 also shows the structural basis of asphaltenes being displaced by EC. Asphaltene molecules are composed of fused aromatic sheets connected by aliphatic chains, with polar functional groups and heteroatoms dotted in the side chains.[39−42] However, the distribution of polar groups on asphaltenes is not dense and uniform, but rather separated by large hydrophobic building blocks such as fused aromatic sheets. When adsorbing on the hydrophilic silica and alumina surfaces, the asphaltene layer cannot occupy all the binding sites on a solid surface, providing opportunities for sequential adsorption of EC. Compared with asphaltenes, the polar (e.g., hydroxyl) binding groups on EC molecules are more uniformly distributed along the polymeric chains and of higher density. As a result, each EC molecule can form multiple bonding with the hydrophilic solid surfaces. With these structural characteristics, the EC molecules, once adsorbed, are expected to lie on the solid surface, although tails and loops of EC chains can also be present (leading to higher dissipation shown in Figures 4 and 6). The structural differences between asphaltenes and EC can be seen in AFM images (Figure 8), where asphaltenes are in the form of randomly distributed nanoaggregates on the silica surface while the silica surface with EC is much more smooth and flatter. Once EC molecules penetrate through the asphaltene layer and bind to the solid surface, they "grab" the solid surface more tightly than asphaltenes due to their higher number of binding sites per EC molecule. In this manner, the adsorbed EC gradually expands to compete for more binding sites on the solid surface and pushes away the neighboring asphaltenes. The driving force for EC to displace the adsorbed asphaltenes is therefore attributed to its higher number of stronger hydrogen bonding sites toward hydroxyl groups on hydrophilic solid surfaces as shown in Figure 10.

From the AFM images (Figure 8c) we know that the displacement of asphaltenes by EC is irreversible and asphaltenes adsorb on EC surface as separate aggregates. Basically, asphaltenes adsorb onto hydrophilic silica or alumina surfaces through polar−polar bonding between asphaltene molecules and the hydrophilic solid surfaces. However, once EC is adsorbed on a hydrophilic solid surface, most of the binding sites on the solid surface would be occupied by EC. Although there are still polar groups on the EC surface that allow polar−polar bonding between asphaltenes and EC, the large hydrophobic block of asphaltene molecules and the ethoxyl chains on EC molecules prevent effective polar−polar bonding between asphaltenes and EC, leaving opportunity mainly for physisorption of asphaltenes on EC surface. The physically adsorbed asphaltenes cannot be easily removed by toluene rinsing because the relatively large size of the adsorbed asphaltene aggregates enables greater van der Waals attractions between asphaltenes and the EC surface. These observations also imply that interactions between asphaltenes and EC play an insignificant role in determining the final occupation of silica surfaces. It is the competition for the hydrophilic binding sites on the silica surface that induces the displacement of asphaltenes by EC. Higher surface affinity of EC ensured its occupation of hydrophilic silica and alumina surfaces.

Effect of EC on Water Wettability of Silane-Treated Hydrophobic Silica Surfaces. The contact angle of water on the silanized hydrophobic silica surfaces before and after immersing in EC-in-toluene solution for 12 h is given in Table 2. As can be seen, the contact angle of water on freshly silanized silica surfaces increased with the number of carbons in alkylchlorosilanes. Upon exposure to 130 ppm EC-in-toluene solution for 12 h, the contact angles of water on all the hydrophobized surfaces decreased to 60−70°. This substantial decrease indicates some adsorption of EC on hydrophobized silica surfaces. Furthermore, if the EC-adsorbed surface was sonicated in 130 ppm EC-in-toluene solution for 1 min, the contact angle of water on the resultant surface returned almost to the value of the original silanized-silica surfaces. This observation indicated weak adsorption of EC on salinized silica surfaces, a characteristic of physisorption. Lack of specific binding, such as hydrogen bond between EC and silanized silica surfaces of methyl-terminal chemistry is responsible for the weak physisorption.

Figure 11 shows topographical images of the butyltrichlorosilane-treated silica surface and of EC adsorbed on the silanized silica surface. The freshly silanized silica surface shows a relatively flat and featureless image. In comparison, EC on silanized silica wafer surfaces has a network structure with an almost constant height of the chains of EC network. This feature is absent for EC adsorbed on a hydrophilic surface (Figure 8c) where a flat surface was observed. On the silanized silica surface, however, there are no polar binding sites and EC molecules tend to fold their polar groups through intra- and intermolecular interactions, leading to the formation of an associated network and a physisorption of

Table 2. Contact Angle of Hydrophobized Silica Surface Treated with EC

	contact angle, deg		
silane type	clean hydrophilic silica surface	silanized (S-) silica	S-silica treated with EC-in-toluene solution
dimethyldichlorosilane	<10	80.9 ± 0.8	67.7 ± 1.5
butyltrichlorosilane		96.6 ± 0.3	62.8 ± 3.3
octyltrichlorosilane		102.1 ± 0.7	67.5 ± 1.3

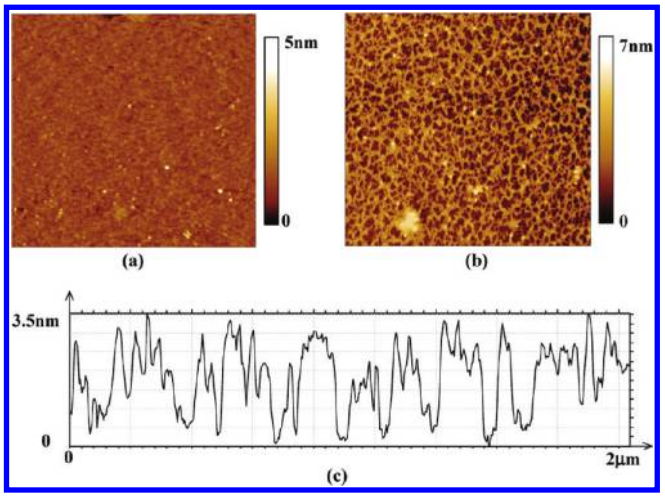

Figure 11. AFM image of (a) butyltrichlorosilane-treated silica surface and (b) EC on butyltrichlorosilane-treated silica surface, and (c) height profile of EC image in (b). The dimension of the images is 2 μm × 2 μm.

EC. In general, through physical adsorption, EC can increase the water wettability, i.e., smaller contact angle, of the silanized silica surface to an intermediate degree. Clearly stronger, multipoint specific bonding (anchoring) of EC with solid surfaces is the key to controlling the wettability of contaminated solids and their behavior in colloidal systems, such as solids-stabilized emulsions.

Solids Removal with EC Addition in Froth Treatment in Oil Sands Processing—Correlation with Current Study. Due to increased water wettability under the influence of EC adsorption, asphaltene- or bitumen-coated fine solids become more hydrophilic and thereby have lower potential in stabilizing water-in-oil emulsions. It was shown by Feng et al.[13] that EC was an effective demulsifier for bitumen froth (essentially a 5 wt % water-in-naphtha diluted bitumen emulsion stabilized by asphaltenes and fine solids) that contains 10 wt % fine solids. They noted that significant amounts of fine solids settled with the coalesced water to the bottom of the emulsions in a graduated cylinder. Some of these fine solids were associated with the emulsified water droplets (e.g., solids at the water−oil interface). For weathered ores containing a large percentage of oil-contaminated solids, EC was shown to be less effective in water removal. It is assumed that solids consumed considerable amount of EC since higher dosage of EC was required for effective water removal.[13] This observation implies that EC acts at both water−oil and solid−oil interfaces, which is desirable for preventing rag layer formation, since rag layer is a complex, interconnected mixture of flocculated fine solids, water droplets, and multiple emulsions.[11,12] However, further investigation is needed on this topic to better correlate the aforementioned results of solid wettability modification by EC with preventing the formation or breaking of rag layers. Such correlation is necessary since in industrial operations much more concentrated asphaltene or bitumen solutions are dealt with. The current study provides a mechanistic insight on the applicability of using chemical modifiers to control the solid wettability in heavy oil phase, by using very dilute solutions of asphaltenes or bitumen in order to obtain clear observation of the displacement process through the analytical equipment, especially AFM.

CONCLUSIONS

In this study, ethyl cellulose (EC), an effective demulsifier for water-in-diluted bitumen emulsions, was shown to decrease the surface hydrophobicity of organic-contaminated solids. The soaking experiments with AFM imaging and contact angle measurement showed that the preadsorbed asphaltenes/bitumen on hydrophilic silica/alumina was displaced by EC in toluene solution. During the displacement by EC, asphaltenes and bitumen were compressed by EC to form a heterogeneous layer of larger aggregates. These aggregates were sparsely scattered on the surface while EC covered most of the solid surface. The displacement occurred because of the higher number of hydroxyl groups per EC molecule and thus a stronger affinity to the hydrophilic solid surface than asphaltenes. The interaction between EC and asphaltenes/bitumen played a minimal role in asphaltene/bitumen displacement by EC. The EC-dominated surface became more hydrophilic and thus can potentially facilitate the solid removal from the oil phase during heavy oil processing. EC adsorption on the silanized hydrophobic silica surface resulted in an intermediate water contact angle of 60−70°. The major findings from this study shed light on controlling the wettability of organic-contaminated solids using chemicals, especially appropriate demulsifiers of w/o emulsions, to improve processability of heavy oils.

AUTHOR INFORMATION

Corresponding Author
*E-mail: zhenghe.xu@ualberta.ca.

ACKNOWLEDGMENT

This work was supported by the Natural Sciences and Engineering Research Council of Canada (NSERC) under the Industrial Research Chair Program in Oil Sands Engineering. We thank Syncrude Canada, Ltd., for providing bitumen sample.

REFERENCES

(1) Feng, X, M. P.; Gao, S; Wang, S; Wu, S. Y.; Masliyah, J. H.; Xu, Z. *Langmuir* **2010**, *26*, 3050.
(2) Sigal, G. B.; Mrksich, M.; Whitesides, G. M. *J. Am. Chem. Soc.* **1998**, *120*, 3464.

(3) Elwing, H.; Welin, S.; Askendal, A.; Nilsson, U.; Lundstrom, I. *J. Colloid Interface Sci.* **1987**, *119*, 203.
(4) Li, X. Y.; Du, X.; He, J. H. *Langmuir* **2010**, *26*, 13528.
(5) Cheng, Y. T.; Rodak, D. E.; Wong, C. A.; Hayden, C. A. *Nanotechnology* **2006**, *17*, 1359.
(6) Sparks, B. D.; Kotlyar, L. S.; O'Carroll, J. B.; Chung, K. H. *J. Pet. Sci. Eng.* **2003**, *39*, 417.
(7) Sjoblom, J.; Aske, N.; Auflem, I. H.; Brandal, O.; Havre, T. E.; Saether, O.; Westvik, A.; Johnsen, E. E.; Kallevik, H. *Adv. Colloid Interface Sci.* **2003**, *100*, 399.
(8) Angle, C. W. *Encyclopedic handbook of emulsion technology*; Sjöblom, J., Ed.; Marcel Dekker, Inc.: New York, 2001.
(9) Saadatmand, M.; Yarranton, H. W.; Moran, K. *Ind. Eng. Chem. Res.* **2008**, *47*, 8828.
(10) Gu, G.; Zhang, L.; Xu, Z.; Mashyah, J. *Energy Fuels* **2007**, *21*, 3462.
(11) Czarnecki, J.; Moran, K.; Yang, X. L. *Can. J. Chem. Eng.* **2007**, *85*, 748.
(12) Romanova, U. G.; Yarranton, H. W.; Schramm, L. L.; Shelfantook, W. E. *Can. J. Chem. Eng.* **2004**, *82*, 710.
(13) Feng, X. H.; Xu, Z. H.; Masliyah, J. *Energy Fuels* **2009**, *23*, 451.
(14) Bensebaa, F.; Kotlyar, L. S.; Sparks, B. D.; Chung, K. H. *Can. J. Chem. Eng.* **2000**, *78*, 610.
(15) Kotlyar, L. S.; Sparks, B. D.; Woods, J. R.; Chung, K. H. *Energy Fuels* **1999**, *13*, 346.
(16) Kotlyar, L. S.; Sparks, B. D.; Woods, J. R.; Raymond, S.; Le Page, Y.; Shelfantook, W. *Pet. Sci. Technol.* **1998**, *16*, 1.
(17) Kotlyar, L. S.; Sparks, B. D.; Woods, J.; Capes, C. E.; Schutte, R. *Fuel* **1995**, *74*, 1146.
(18) Wu, X. A. *Energy Fuels* **2008**, *22*, 2346.
(19) Sztukowski, D. M.; Yarranton, H. W. *J. Colloid Interface Sci.* **2005**, *285*, 821.
(20) Sztukowski, D. M.; Yarranton, H. W. *J. Dispersion Science Technol.* **2004**, *25*, 299.
(21) Sullivan, A. P.; Kilpatrick, P. K. *Ind. Eng. Chem. Res.* **2002**, *41*, 3389.
(22) Vander Kloet, J.; Schramm, L. L.; Shelfantook, B. *Colloids Surf., A* **2001**, *192*, 15.
(23) Poindexter, M. K.; Marsh, S. C. *Energy Fuels* **2009**, *23*, 1258.
(24) Ekholm, P.; Blomberg, E.; Claesson, P.; Auflem, I. H.; Sjoblom, J.; Kornfeldt, A. *J. Colloid Interface Sci.* **2002**, *247*, 342.
(25) Zhang, L. Y.; Lawrence, S.; Xu, Z. H.; Masliyah, J. H. *J. Colloid Interface Sci.* **2003**, *264*, 128.
(26) Slavov, S. V.; Chuang, K. T.; Sanger, A. R. *J. Phys. Chem.* **1996**, *100*, 16285.
(27) Hannisdal, A.; Ese, M. H.; Hemmingsen, P. V.; Sjoblom, J. *Colloids Surf., A* **2006**, *276*, 45.
(28) Hook, F.; Rodahl, M.; Brzezinski, P.; Kasemo, B. *Langmuir* **1998**, *14*, 729.
(29) Rodahl, M.; Hook, F.; Fredriksson, C.; Keller, C. A.; Krozer, A.; Brzezinski, P.; Voinova, M.; Kasemo, B. *Faraday Discuss.* **1997**, *107*, 229.
(30) Richter, R. P.The Formation of Solid-Supported Lipid Membranes and Two-Dimensional Assembly of Proteins.*Thesis*, Université Bordeaux I—Institut Européen de Chimie et Biologie, 2004
(31) Abudu, A.; Goual, L. *Energy Fuels* **2009**, *23*, 1237.
(32) Dudasova, D.; Silset, A.; Sjoblom, J. *J. Dispersion Sci. Technol.* **2008**, *29*, 139.
(33) Volden, S.; Zhu, K. Z.; Nystrom, B.; Glomm, W. R. *Colloids Surf., B* **2009**, *72*, 266.
(34) Wang, S. Q.; Liu, J. J.; Zhang, L. Y.; Xu, Z. H.; Masliyah, J. *Energy Fuels* **2009**, *23*, 862.
(35) Franks, G. V.; Meagher, L. *Colloids Surf., A* **2003**, *214*, 99.
(36) Sztukowski, D. M.; Yarranton, H. W. *Langmuir* **2005**, *21*, 11651.
(37) Bouriat, P.; El Kerri, N.; Graciaa, A.; Lachaise, J. *Langmuir* **2004**, *20*, 7459.
(38) Freer, E. M.; Radke, C. J. *J. Adhes.* **2004**, *80*, 481.
(39) Mullins, O. C.; E. Y. S., Hammami, A.; Marshall, A. G. *Asphaltenes, heavy oils, and petroleomics*; Springer: New York, 2007.
(40) Sheremata, J. M.; Gray, M. R.; Dettman, H. D.; McCaffrey, W. C. *Energy Fuels* **2004**, *18*, 1377.
(41) Strausz, O. P.; Mojelsky, T. W.; Lown, E. M. *Fuel* **1992**, *71*, 1355.
(42) Dickie, J. P.; Yen, T. F. *Anal. Chem.* **1967**, *39*, 1847.